Enhanced memory function after septo-hippocampal stimulation by focused ultrasound in a mouse model of Alzheimer's disease

Younghee Seo

Department of Medical Science

The Graduate School, Yonsei University

Enhanced memory function after septo-hippocampal stimulation by focused ultrasound in a mouse model of Alzheimer's disease

Directed by Professor Jin Woo Chang

The Doctoral Dissertation
submitted to the Department of Medical Science,
the Graduate School of Yonsei University
in partial fulfillment of the requirements for the degree of
Doctor of Philosophy in Medical Science

Younghee Seo

December 2023

This certifies that the Doctoral Dissertation of Younghee Seo is approved.

Thesis Supervisor: Jin Woo Chang

Thesis Committee Member #1: Bae Hwan Lee

Thesis Committee Member #2: Won Seok Chang

Thesis Committee Member #3: Hyungmin Kim

Thesis Committee Member #4: Chang Kyu Park

The Graduate School
Yonsei University

December 2023

ACKNOWLEDGEMENTS

I want to express my sincere gratitude to all those who supported and encouraged me. First, I deeply appreciate Prof. Jin Woo Chang, who consistently provided unwavering support, enabling me to engage in research across various fields. His guidance as a pioneering researcher in neurosurgery, leading basic and clinical studies, has instilled in me a great sense of pride and inspiration. Thanks to his excellent mentorship, I have learned a great deal during this Ph.D. study, and I will continue to progress with gratitude.

I would also like to extend my heartfelt gratitude to Prof. Bae Hwan Lee, Prof. Hyungmin Kim, and Prof. Chang Kyu Park for their insightful advice and encouragement. Especial thanks to the guidance of Prof. Won Seok Chang, I have grown and learned more through the experiences and time spent in the laboratory.

I express my special thanks to Prof. Young Cheol Na, who provided diverse research opportunities, Prof. Bong Soo Kim, who encouraged me warmly, Prof. Byeong-Wook Song, who provided helpful experimental discussions, and Prof. Hyun Ho Jung, who always greeted me amicably.

To my colleagues in my NSIM laboratory, I extend my gratitude and best wishes. I will cherish the memories we shared and continue to support each of you. I also extend thanks to Dr. Chin Su Koh, Dr. Jaewoo Shin, Dr. Chanho Kong, Dr. Minkyung Park, Jiyeon Sim, Junwon Park, Ji Young Park, Jiwon Baek, Heesue Chang, Tae Jun

Kim, Won Ki Mun, Seung Hyun Min, Shinyeong Oh, and Hyeon Ju Lee. Also, a special thanks to Sangheon Han for helping me enthusiastically to complete this research. In addition, I would like to express my gratitude to Dr. Jihyeon Lee, who has been with me since the beginning of my graduate school studies, always supporting me and being a source of strength during challenging times.

To my long-time friends So Hee, Kyungyeon, Hansol, and Sujin, and to my BME friends Suyeon, Minju, Hyungyu, and Duckyoung, I want to convey my heartfelt thanks for your unwavering trust and support.

Lastly, I want to convey my deepest appreciation to my parents, who have always believed in and supported me. Thanks to your boundless love and support, I completed this Ph.D. study. Your faith and encouragement have been valuable lessons for me, and I will strive to repay your love and be a proud daughter.

Meeting all these precious individuals made me realize the value and joy of research. In the future, I will continue to share what I have gained, help others, and relentlessly pursue learning and personal growth.

December 2023

Younghee Seo

TABLE OF CONTENTS

LIST OF FIGURES

LIST OF TABLES

ABSTRACT

Enhanced memory function after septo-hippocampal stimulation by focused ultrasound in a mouse model of Alzheimer's disease

Younghee Seo

Department of Medical Science
The Graduate School, Yonsei University

(Directed by Professor Jin Woo Chang)

Alzheimer's disease (AD) is a progressive neurodegenerative disorder characterized by cognitive decline, memory loss, and behavioral impairments. Current therapeutic approaches for AD focus on symptomatic management, with limited success in modifying disease progression. Therefore, there is an urgent need for innovative interventions that target the underlying pathological mechanisms of AD to preserve or enhance cognitive function.

Focused ultrasound (FUS) has emerged as a promising non-invasive neuromodulation technique with high spatial precision. This research investigated the effects of low-intensity FUS on the septo-hippocampal

area in normal and five familial AD (5xFAD) mouse models to explore its potential for enhancing cognitive function. The septo-hippocampal circuitry plays a crucial role in cognitive processes, and its dysfunction is a prominent feature of AD pathology.

This study treated the septo-hippocampal area using low-intensity FUS, and cognitive function was evaluated through behavioral assessments. Remarkably, normal and AD model subjects exhibited significant cognitive improvements following FUS treatment, indicating its potential as a novel therapeutic strategy for AD. The potential involvement of the brain-derived neurotrophic factor (BDNF) pathway in mediating the observed cognitive enhancements was interrogated to elucidate the underlying mechanisms. BDNF, a key protein in neuronal survival and synaptic plasticity, has been implicated in the pathophysiology of AD. Understanding the interplay between FUS, BDNF, and cognitive function provides valuable insights into the potential therapeutic mechanisms of FUS-based interventions.

This study's findings suggest that the FUS neuromodulation of the septo-hippocampal area holds promise for enhancing cognitive function in AD. By offering a non-invasive and precise approach to modulating brain activity, FUS presents a potential disease treatment.

This study contributes to the growing body of evidence supporting FUS as a viable treatment option for AD and fosters hope for individuals affected by this disease. By investigating the impact of FUS on the septo-hippocampal area of the brain and exploring potential molecular pathways, these findings pave the way for developing targeted and effective therapeutic strategies to improve cognitive function in AD and other neurological disorders.

Key words: alzheimer's disease, focused ultrasound, septo-hippocampal pathway, brain-derived neurotrophic factor, cognitive function

Enhanced memory function after septo-hippocampal stimulation by focused ultrasound in a mouse model of Alzheimer's disease

Younghee Seo

Department of Medical Science
The Graduate School, Yonsei University

(Directed by Professor Jin Woo Chang)

I. INTRODUCTION

Alzheimer's disease (AD) is a devastating neurodegenerative disorder characterized by progressive cognitive decline, memory impairment, and behavioral disturbances.[1,2] As the global population ages, the prevalence of AD continues to rise, presenting a substantial challenge for healthcare systems worldwide.[3,4] Current therapeutic approaches for AD primarily focus on managing symptoms and providing temporary relief, with limited success in modifying the underlying disease process.[5,6] As a result, there is an urgent need for innovative interventions that target the fundamental pathological mechanisms of AD, aiming to preserve or even enhance cognitive function.

In recent years, neuromodulation techniques have emerged as promising avenues for treating AD.[7-9] Among these techniques, focused ultrasound (FUS) has gained considerable attention as a non-invasive modality capable of

precisely targeting specific brain regions with high spatial resolution.[10,11] By focusing ultrasonic waves through the intact skull, FUS enables precise and controlled neuromodulation without the need for invasive procedures or the administration of exogenous substances.[12,13] In addition, FUS modulation has shown potential for influencing neural activity, offering a novel approach to address the intricate brain circuitry implicated in AD pathogenesis.[14] The ability to non-invasively and precisely target brain regions holds significant advantages over traditional interventions, which often have substantial risks and limited precision.[15] The focused ultrasonic waves can be applied with high accuracy to stimulate or inhibit specific neural populations, thereby modulating neuronal network activity in a controlled manner.[16,17] Moreover, FUS allows for repeated and reversible neuromodulation, presenting a unique advantage for personalized treatment strategies and potentially reducing the risk of adverse effects associated with irreversible interventions.[18,19] This adaptability opens the door to tailored therapeutic protocols that can be adjusted based on individual responses and disease progression. Additionally, FUS may offer a safer alternative to invasive techniques, making it more accessible to a broader range of patients, including those who might not be suitable candidates for surgical interventions due to various health conditions or age-related factors.

In the context of AD, the septo-hippocampal area holds particular significance. The septo-hippocampal circuitry plays a crucial role in cognitive processes, including learning and memory.[20,21] Dysfunction and degeneration

within this circuitry are prominent features of AD pathology.[22] Therefore, targeting the septo-hippocampal area for neuromodulation presents a compelling opportunity to enhance cognitive function in AD.

Additionally, the role of brain-derived neurotrophic factor (BDNF) pathways in mediating the cognitive enhancements after FUS treatment has been explored. BDNF, a critical protein involved in neuronal survival and synaptic plasticity, has been implicated in the pathophysiology of AD.[23-25] Therefore, understanding the interplay between FUS, BDNF, and cognitive function could shed light on the therapeutic mechanisms underlying FUS-based interventions. Another advantage of FUS is that, in addition to spatial precision, it can modulate brain activity at various levels, from neural circuits to molecular pathways.[26] Among these pathways, the BDNF pathway has garnered significant attention in AD research due to its role in promoting neuronal survival, synaptic plasticity, and cognitive function.[27] Our exploration of the specific connection between FUS and the BDNF pathways may uncover novel and effective approaches to utilize FUS for AD treatment, thus advancing our comprehension of the complex mechanisms underlying cognitive improvement.

The aim of this research was to investigate the impact of low-intensity FUS on the septo-hippocampal area and its effect on cognitive function, in a normal and five familial AD (5xFAD) mouse model of Alzheimer’s disease. The 5xFAD mice, characterized by the overexpression of amyloid beta, which is one feature of Alzheimer's disease, express five mutations responsible for the

accumulation and increase in amyloid beta plaques.[28] By utilizing FUS as a neuromodulation tool, the potential to improve cognitive function by leveraging the inherent capacity of FUS to influence neural circuitry and promote neuroprotection in the targeted brain regions was studied. Additionally, this study aimed to explore the use of FUS as a neuromodulation tool for AD, with a specific focus on leveraging BDNF pathways to enhance cognitive function.

This study elucidated FUS neuromodulation and its role in enhancing cognitive function in normal and AD mouse models. By investigating the impact on the septo-hippocampal area and exploring potential molecular pathways, the study's findings have the potential to influence the development of targeted and effective therapeutic strategies for AD, offering hope for individuals affected by this disease.

II. MATERIALS AND METHODS

Part 1. Effects of FUS stimulation on memory improvement

1. Experimental animals

All animal experiments were performed in accordance with the Guide for the Care and Use of Laboratory Animals of the National Institutes of Health and approved by the Institutional Animal Care and Use Committee of Yonsei University, Korea (IACUC number: 2023-0148). The male C57BL/6 mice (25–30 g) were housed in groups of five per cage in a temperature/ humidity-controlled room with a 12/12 hr light/dark cycle and were provided with *ad libitum* access to food and water. Every effort was made to minimize the number of mice used and overall animal suffering.

2. The FUS parameters

Experimental mice were anesthetized with 5% isoflurane in oxygen. After fixing the mouse on the stereotaxic frame, the scalp was incised, and the medial septum (MS) (Anteroposterior [AP] = +0.6 mm, mediolateral [ML] = 0) and hippocampus (HP) (AP = −2 mm, ML = ±1.3 mm) were located based on the bregma. Next, the transducer, along with a water tank containing degassed water, were placed on the area, ultrasound gel was applied, and the ultrasound was sonicated (Figure 1).

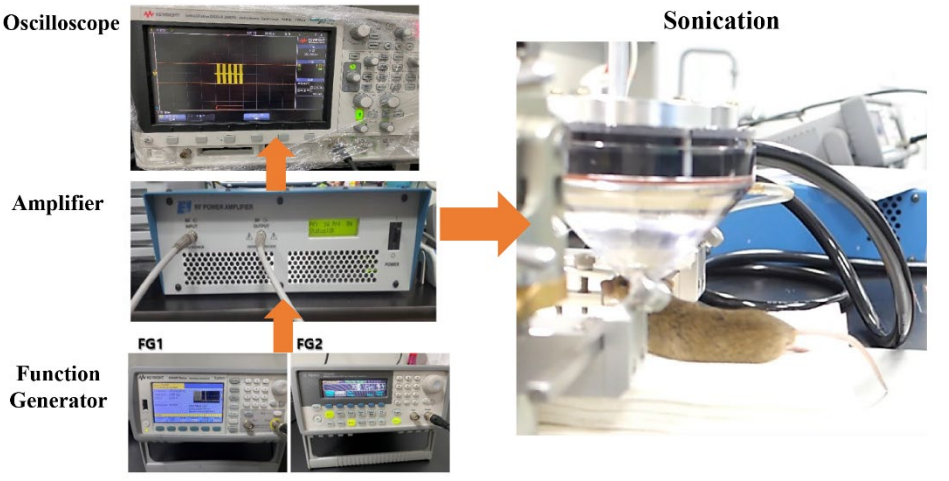

Figure 1. Schematic diagram of the focused ultrasound (FUS) system.

First, the function generator controlled the pulse repetition frequency (PRF), sonication duration (SD), and inter-stimulus interval (ISI) by triggering the operation of the second function generator, which controlled the ultrasound fundamental frequency (FF), tone-burst duration (TBD), and acoustic intensity (AI). Sonication parameters of 515 kHz FF, 50% duty cycle (DC), 300 ms SD, and 2 s ISI were used, and the PRF was varied and compared at 30, 300, 1000, 2500, and 4000 Hz to optimize the parameters (Figure 2).

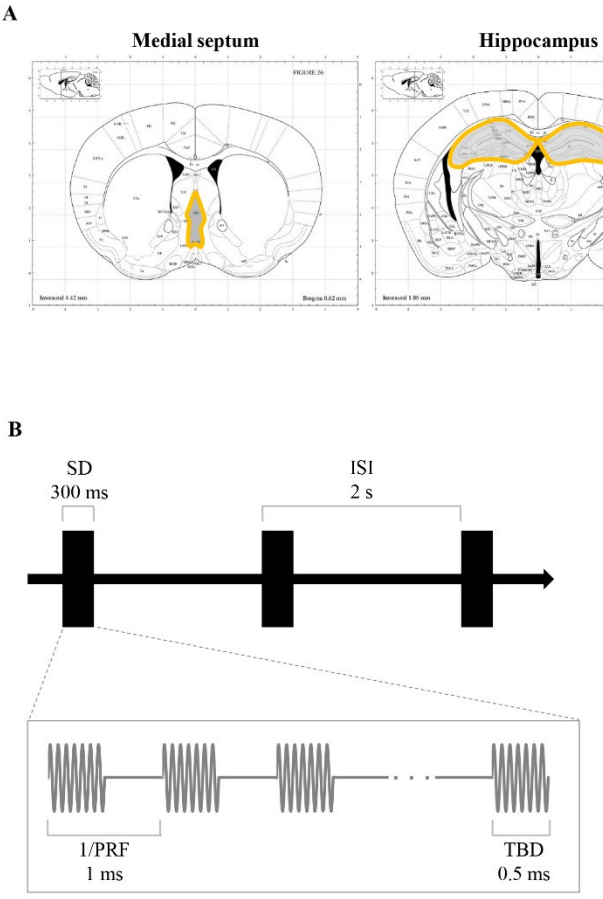

Figure 2. Sonication regions and parameters modulated by function generators. (A) Sonication regions. (B) The sonication parameters included a sonication duration of 300 ms, inter-stimulus interval of 2 s, pulse repetition frequency of 1 kHz, tone-burst duration of 0.5 ms, duty cycle of 50%, and a total sonication time of 40 min.

3. Efficacy and safety of FUS modulation

To determine the efficacy of FUS according to changes in sonication PRF, the animals were divided into five groups: Group 1 (PRF 30 Hz), Group 2 (PRF 300 Hz), Group 3 (PRF 1000 Hz), Group 4 (PRF 2500 Hz), and Group 5 (PRF 4000 Hz), where n = 10 for each group.

The expression of c-fos, a neuronal activity marker, and BDNF, a neurotrophic factor marker, was evaluated by western blotting (n = 7 per group) and immunohistochemistry (n = 3 per group). Co-immunostaining of BDNF and glial fibrillary acidic protein (GFAP) was confirmed, and hematoxylin and eosin (H&E) staining was performed to confirm brain damage.

Mechanosensitive ion channel expression was confirmed to prove the FUS stimulation site. The mechanosensitive ion channel of large conductance (MscL)-G22S virus (rAAV-hsyn-MSCL-G22S-F2A-EYFP-WPRE-pA, AAV2/9) was used, which works following the same principle as GCaMP6 and is characterized by only excited neurons expressing fluorescence when stimulated.[29] Viruses were injected into the MS (n = 3) and right HP (n = 3) at 1 μL each, and the FUS was sonicated 5 weeks after virus injection considering the expression time of the AAV virus.

4. Treatment with FUS

The groups were divided into a total of four groups: a control group and three FUS groups. The FUS groups were as follows: FUS-stimulated on the MS, FUS-stimulated on the HP, and FUS-stimulated on the MS + HP.

To demonstrate the most effective stimulation site among the FUS groups (n = 12 per group), a western blot was performed (n = 7 per group) for BDNF and tropomyosin receptor kinase B (TrkB) detection according to BDNF signaling, and the expression of N-methyl D-aspartate receptor subtype 2B (NR2B) was also confirmed through western blot to confirm the change in synaptic N-methyl-D-aspartate (NMDA) receptors. In addition, BDNF and GFAP were identified by co-immunostaining (n = 5 per group).

5. Behavioral test: Spontaneous alteration in the Y-maze

To investigate cognition and spatial memory after 2 days of FUS treatment, spontaneous alternation in the Y-maze (n = 12 per group) was assessed. The maze was constructed of black opaque acrylic with three arms of equal size and height (40 × 15 × 9 cm) arranged in a Y shape. All mice were placed one by one in the center of the maze and their alternation movements were recorded with a camera for 8 min. Analysis of the alternation ratios was performed by determining whether the animals alternately entered the three arms.

Part 2. Modulation of the septo-hippocampal pathway in a 5xFAD mouse model of AD

6. Alzheimer's disease model

The 5xFAD mouse expresses five mutations that accumulate and increase beta-amyloid (Aβ) plaques: Swedish (KM670/671NL), Florida (I716V), and London (V717I) mutations in amyloid precursor protein (APP), and M146L and L286V mutations in presenilin-1 (PSEN1). This mouse is a transgenic model maintained in the B6SJL background in a hemizygous state and shows stable transmission and expression across generations. Genotyping was carried out using a 2% agarose gel polymerase chain reaction (PCR) analysis of the ear tissue DNA to confirm the presence of the human APP and PSEN1 transgenes. Transgenic mice were identified using the primer sequences in Table 1. Only individuals expressing both PSEN1 (608 bp) and APP (377 bp) were used in the experimental group as transgenic (TG), and non-transgenic littermates (LM) were used as controls (Figure 3A).

The significant amyloid pathology in the 5xFAD model appears rapidly. High quantities of intraneuronal Aβ42 accumulate in these mice starting at 1.5 months of age[28]. An assessment of spatial working memory called the Y-maze spontaneous alternation test shows impairment starting at about 4 to 5 months of age[30]. In this model, neuron loss has also been shown at about 6 months of age in several brain areas[31].

Male 5–6-month-old 5xFAD mice weighing about 20–30 g were used. The amyloid plaques of TG mice used in this study were also confirmed (Figure 3B). All animal experiments were performed in accordance with the Guide for the Care and Use of Laboratory Animals of the National Institutes of Health and approved by the Institutional Animal Care and Use Committee of Yonsei University, Korea (IACUC number: 2023-0148).

Table 1. Primer sequences

Gene	Primer sequence (5'-3')	Product size (bp)
PSEN1	forward: AAT AGA GAA CGG CAG GAG CA reverse: GCC ATG AGG GCA CTA ATC AT	608
APP	forward: AGG ACT GAC CAC TCG ACC AG reverse: CCG GGG TCT AGT TCT GCA T	377
GAPDH	forward: AGG TCG GTG TGA ACG GAT TTG reverse: TGT AGA CCA TGT AGT TGA GGT CA	123

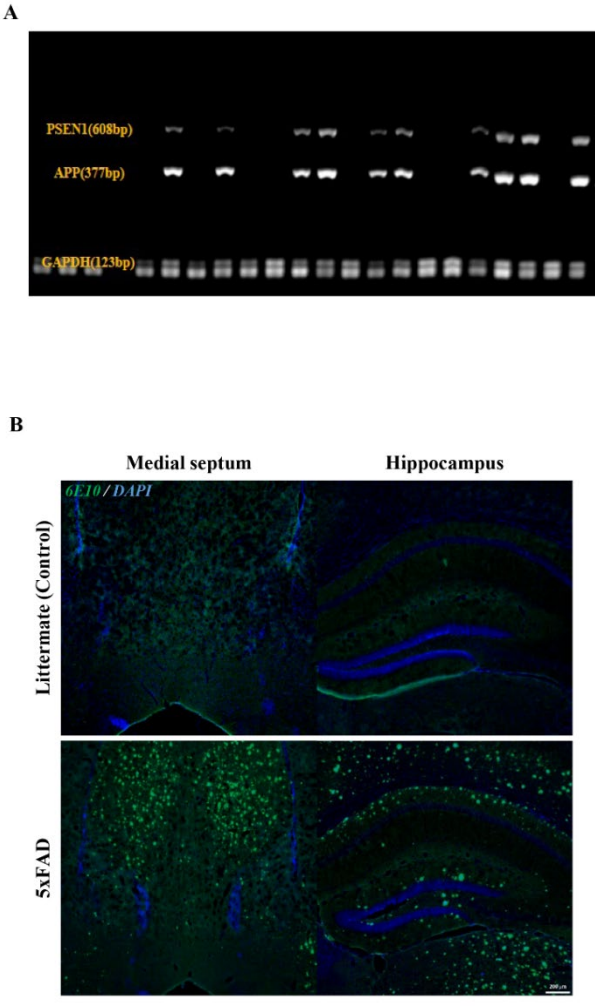

Figure 3. Verification of 5xFAD mice with genotyping PCR and beta-amyloid (Aβ) accumulation. (A) Genotyping PCR for amyloid precursor protein (APP) and presenilin-1 (PSEN1) in 5xFAD mice. (B) As a result of medial septum and hippocampus area staining using the anti-Aβ 6E10 antibody, Aβ accumulation in 5xFAD mice was confirmed. The scale bar represents 200 μm.

7. The FUS system for the septo-hippocampal pathway

Experimental mice were anesthetized with 5% isoflurane in oxygen. The experimental group was divided into three groups of mice: littermate control (LM, n = 12), transgenic (5xFAD) (TG, n = 12), and TG with stimulated septo-hippocampal regions using FUS (TG + FUS, n = 60). The scalp was incised once the mouse was secured to the stereotaxic frame. The FUS system consisted of a 515 kHz single-element spherically focused H-107MR transducer (Sonic Concept Inc., Bothell, WA, USA), two waveform generators (33600A, 33500B; Keysight, Santa Rosa, CA, USA), and a radiofrequency power amplifier (240 L; ENI Inc., Rochester, NY, USA). The parameters used were as follows: 515 kHz FF, 50% DC, 1 kHz PRF, 0.5 ms TBD, 300 ms SD, and 2 s ISI. Animals in the TG + FUS group were stimulated at the MS (coordinates from bregma: AP + 0.6, ML 0 mm) and bilateral HP sites (coordinates from bregma: AP -2, ML ±1.3 mm) for a total of 40 min. The FUS-treated animals were sacrificed after the Y-maze test at 1 hour, 1 day, 2 days, 3 days, and 4 days (Figure 4).

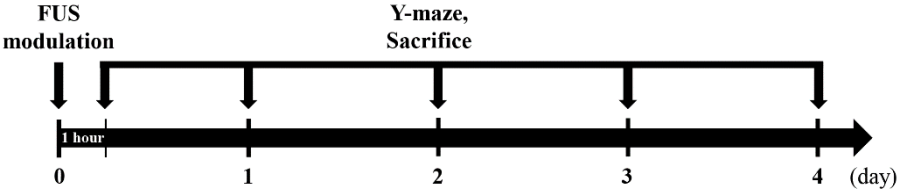

Figure 4. Experimental timeline for FUS modulation in 5xFAD mice. Mice were sacrificed after the implementation of the Y-maze test at 1 hour, 1 day, 2 days, 3 days, and 4 days, respectively, following the FUS treatment.

8. Behavioral test: Spontaneous alteration in the Y-maze

Spontaneous alternation in the Y-maze (n = 12 for each group) was used in the LM, TG, and TG + FUS groups (1 hour, 1 day, 2 days, 3 days, and 4 days after FUS) to investigate cognition and spatial memory. The maze was composed of black opaque acrylic with three arms of equal size and height (40 × 15 × 9 cm) arranged in a Y shape. All mice were placed one by one in the center of the maze and their alternation movements were recorded with a camera for 8 min. The alternation ratios were calculated by assessing whether the animals entered the three arms alternately.

9. Immunohistochemistry analysis

Animals (n = 5 per group) were anesthetized and perfused with 0.9% saline and 4% paraformaldehyde. The brains were extracted and postfixed in 4% paraformaldehyde (Duksan, Seoul, South Korea) for 3 days at 4°C, then transferred to 30% sucrose (Duksan, Seoul, South Korea) for 3 days at 4 °C, sectioned into 30 μm slices using a cryostat (Leica Biosystems, Wetzlar, Germany), and stored at −20 °C in a cryoprotectant solution containing 0.1 M phosphate buffer (pH 7.2), 30% sucrose, 1% polyvinylpyrrolidone (Sigma-Aldrich, St. Louis, MO, USA), and 30% ethylene glycol (Thermo Fisher Scientific, Waltham, MA, USA).

For fluorescence immunohistochemistry, brain tissues were stored in 0.3% H_2O_2 for 30 min to inactivation endogenous peroxidase activity after washing in

phosphate-buffered saline (PBS). Blocking was conducted with 10% normal goat serum (Vector Labs, Burlingame, CA, USA) for 1 hour. Primary antibodies, BDNF (1:200; Abcam, Cambridge, UK), GFAP (1:400; Abcam, Cambridge, UK), or S100A10 (1:100; Abcam, Cambridge, UK), were incubated with the brain tissues overnight at 4 °C. The next day, the brain tissues were incubated with secondary antibodies conjugated with Alexa Fluor 488 (A11001 or A11039, 1:400; Thermo Fisher Scientific, Waltham, MA, USA) or Alexa Fluor 633 (A21071, 1:200; Thermo Fisher Scientific, Waltham, MA, USA) for 2 hours at room temperature. The staining intensity of the sections were visualized using an LSM 700 confocal microscope (Carl Zeiss, Jena, Germany).

For diaminobenzidine (DAB) staining of choline acetyltransferase (1:100, ChAT; Merck, Darmstadt, Germany), the sections were incubated with biotinylated secondary antibodies, followed by the avidin-biotin complex method (ABC Elite; Vector Labs, Burlingame, CA, USA). They were visualized with DAB using a DAB substrate kit (Thermo, Rockford, IL, USA). Staining of sections was visualized with an optical microscope (BX51; Olympus, Tokyo, Japan).

10. Western blot analysis

The brains of the anesthetized mice (n = 7 per group) were quickly excised for protein extraction. The MS and HP were dissected using fine forceps from 1 mm coronal brain slices. The samples were homogenized in lysis buffer (Intron, Seongnam, Korea) and placed on ice for 30 min. They were then centrifuged for 30 min at 13,000 rpm, and the protein content in the supernatant was then measured using the bicinchoninic acid protein assay reagent kit (Pierce, Rockford, IL, USA). The protein samples were stored at -70°C.

Proteins were separated by 8–15% sodium dodecyl sulfate polyacrylamide gel electrophoresis and transferred onto polyvinylidene fluoride membranes. The membranes were then blocked with 5% skim milk (BD Difco, Franklin Lakes, NJ, USA) in Tris-buffered saline with Triton X-100 (Sigma-Aldrich, St. Louis, MO, USA).

Membranes were incubated with primary antibodies c-fos (1:2000; Abcam, Cambridge, UK), BDNF (Brain-derived neurotrophic factor, 1:2000; Abcam, Cambridge, UK), TrkB (Tropomyosin receptor kinase B, 1:500; Abcam, Cambridge, UK), Akt (1:1000; Proteintech, Rosemont, IL, USA), p-Akt (phosphorylated protein kinase B, 1:1000; Proteintech, Rosemont, IL, USA), NR2B (N-methyl D-aspartate receptor subtype 2B, 1:1000; NeuroMab, Davis, CA, USA), and GAPDH (1:2000; Cell Signaling Technology, Danvers, MA, USA) and stored overnight at 4 °C. The secondary antibody, horseradish peroxidase (HRP)-conjugated goat anti-mouse IgG (H+L) or goat anti-rabbit

IgG (H+L)-HRP (GenDEPOT, Katy, TX, USA), was applied at 25 °C for 2 hours.

The proteins were detected using an enhanced chemiluminescence solution (West Save, Western blot detection kit; Abfrontier, Seoul, South Korea). Signals were obtained using Amersham ImageQuant 800 (GE Healthcare Life Sciences, Chicago, IL, USA). In addition, band signals were evaluated using an analytical system (Multi Gauge version 3.0; Fujifilm, Tokyo, Japan).

11. Acetylcholinesterase assay

The same protein samples that were used for western blotting were also used for this experiment. The enzymatic activity of acetylcholinesterase (AChE) was determined using the method proposed by Ellman et al.[32] with some modifications. At 37°C, triplicate samples (20 μL) were combined with the reaction mixture, which included 0.2 mM dithiobis nitrobenzoic acid (Sigma-Aldrich, St. Louis, MO, USA), 0.56 mM acetylthiocholine iodide (Sigma-Aldrich, St. Louis, MO, USA), 10 μM tetraisopropyl pyrophosphoramide (Sigma-Aldrich, St. Louis, MO, USA), and 39 mM phosphate buffer (pH 7.2). The optical density was measured at 405 nm after 30 min.

12. Statistical analyses

Data were analyzed by one-way analysis of variance (ANOVA) with Tukey's post-hoc comparisons, and statistical analysis was performed using GraphPad Prism 7 (GraphPad Software, Inc., San Diego, CA, USA). Data were presented as the mean ± standard error of the mean. Statistical significance was set at $*P < 0.05$, $**P < 0.01$, $***P < 0.001$, and $****P < 0.0001$.

III. RESULTS

Part 1. Effects of FUS stimulation on memory improvement

1. Verification of brain modulation according to FUS parameters

To determine brain modulation depending on the changes in the PRF in a constant DC of 50%, the expression of c-fos, a neuronal activity marker, was confirmed in response to 30 (Group 1), 300 (Group 2), 1000 (Group 3), 2500 (Group 4), and 4000 (Group 5) Hz. In addition, among the parameters that increase neural activity, the parameter in which BDNF, a neurotrophic factor, increases the most was confirmed. As a result, when the PRF was 1000 Hz, c-fos and BDNF increased the most (Figure 5).

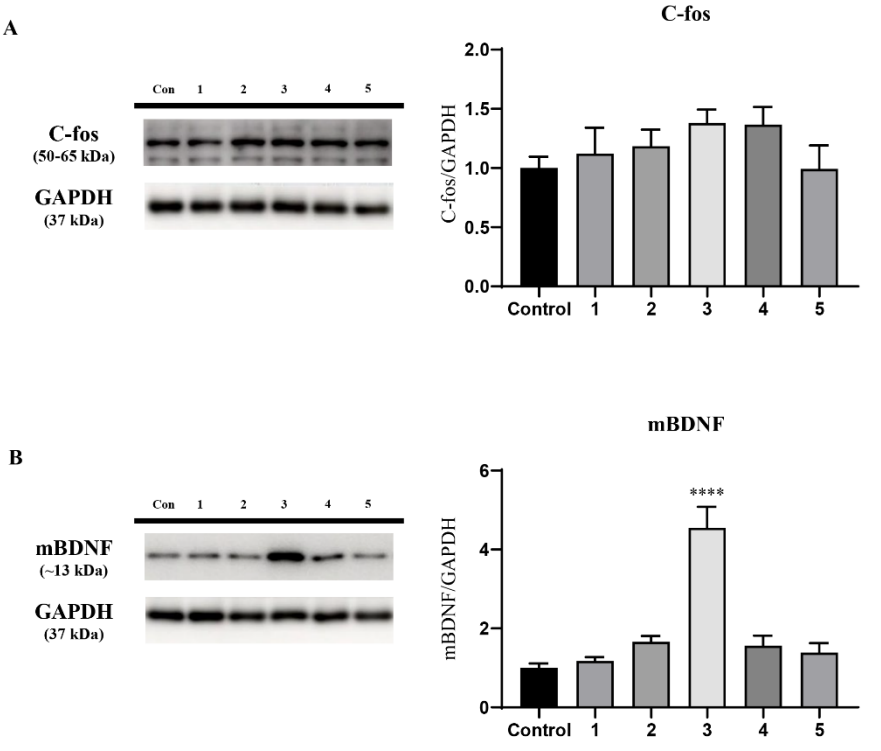

Figure 5. Expression levels of c-fos and mBDNF according to the pulse repetition frequency (PRF). (A) The expression level of c-fos was elevated in the focused ultrasound (FUS) groups. (B) The mBDNF expression level was significantly increased in FUS Group 3 compared to that of the control group (****$p < 0.0001$). Data were expressed as the mean ± standard error of the mean (n = 7 for each group).

FUS using this parameter was used to treat the MS and HP, and mechanosensitive channel expression was confirmed. The MscL virus, which was injected before FUS, is a calcium indicator that can be used to image and measure changes in calcium concentrations associated with neural activity. As a result, it was confirmed that fluorescence was expressed in the targeting area by the MS and HP groups, respectively (Figure 6).

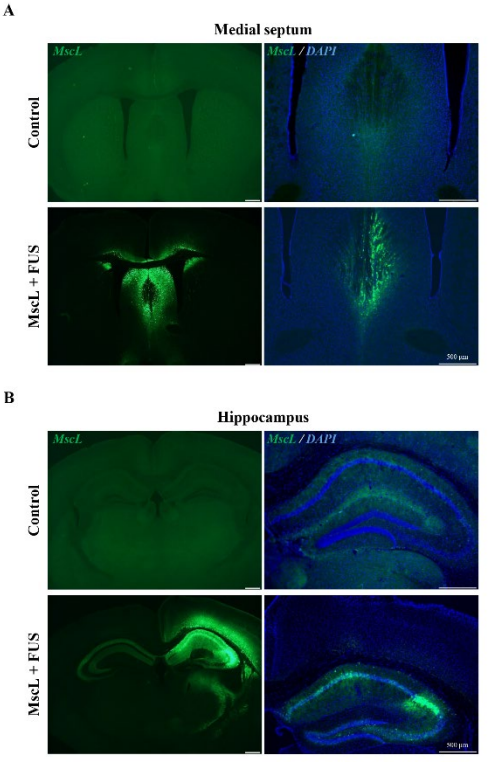

Figure 6. Confirmation of FUS-targeted regions using MscL expression. (A) Expression in the medial septum. (B) Expression in the hippocampus. The scale bar represents 500 μm.

2. Examination of safety of FUS modulation

Evaluation of damage to the brain region by H&E staining revealed no visible structural injuries or extravasated red blood cells in the sonicated brain regions (Figure 7).

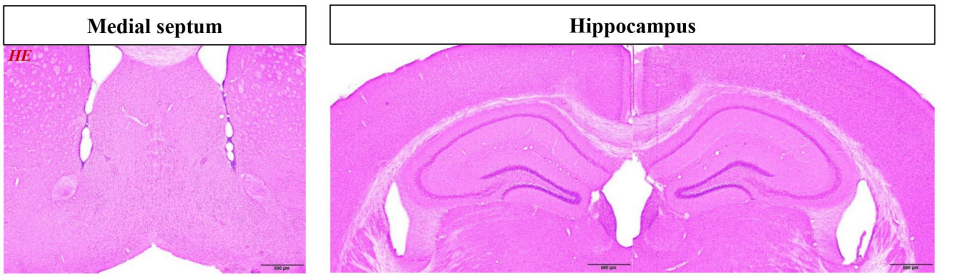

Figure 7. Confirmation of safety of focused ultrasound (FUS) modulation. The sonicated brain regions were histologically evaluated by H&E staining. The scale bar represents 500 μm.

3. Increased BDNF in the astrocytes in the FUS-sonicated region

Changes in BDNF expressed in astrocytes according to PRF parameters were confirmed through immunohistochemistry. As a result, the highest amount of expression was confirmed in group 3 (Figure 8A). When group 3's tissues were enlarged, it was confirmed that the FUS-treated HP had an overall increased expression of BDNF in astrocytes compared to that of the untreated, contralateral sites (Figure 8B). To further confirm the co-expression of astrocytes and BDNF, images at 40× magnification were also taken (Figure 8C).

In addition, the expression of astrocytes according to the phenotype was also confirmed. When the A1 phenotype marker C3 and BDNF were stained together, there was no change in the astrocyte expression in the FUS group compared to that of the control (Figure 9); whereas, when the A2 phenotype marker S100A10 and BDNF were stained together, it was confirmed that astrocyte expression in the FUS group increased compared to that of the control group, and in particular, the largest increase was confirmed in the MS+HP group (Figure 10A; enlarged to 40× magnification in Figure 10B).

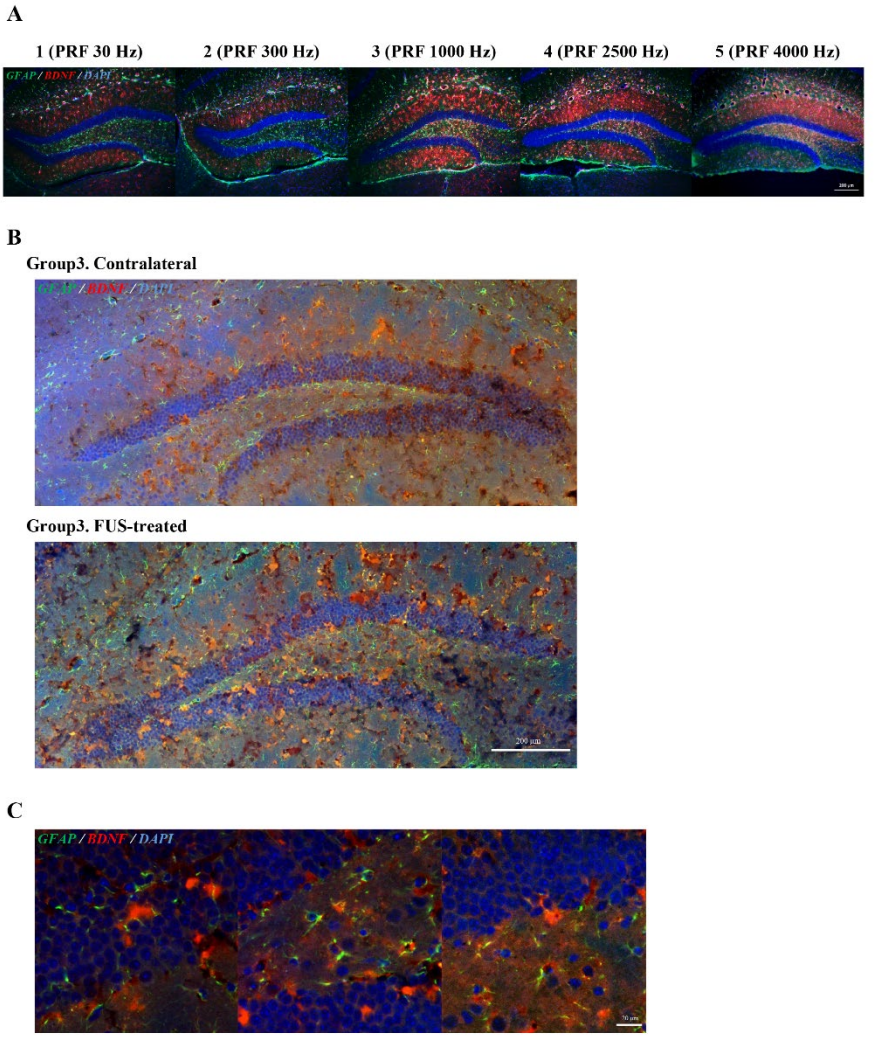

Figure 8. Comparison of BDNF expression in astrocytes. (A) Immunohistochemistry for glial fibrillary acidic protein (GFAP) and brain-derived neurotrophic factor (BDNF) according to pulse repetition frequency (PRF). (B) Untreated and FUS-treated regions of the PRF Group 3. (C) 40× magnification images. The scale bar represents 200 μm (Figures 8A & B) and 20 μm (Figure 8C).

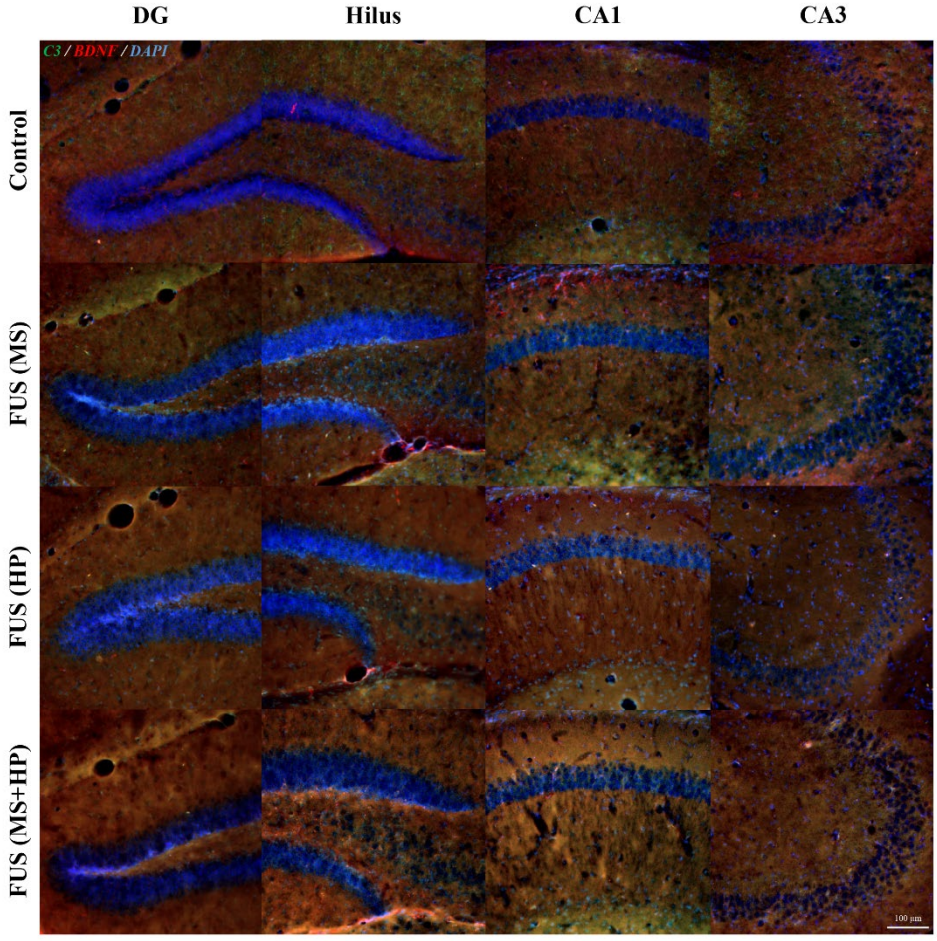

Figure 9. Co-staining BDNF and A1-type astrocytes. There was no change in the astrocyte expression between groups as a result of staining the A1-type astrocyte marker C3 (green) and BDNF (red). The scale bar represents 100 μm. MS: medial septum; HP: hippocampus; MS+HP: medial septum + hippocampus. DG: dentate gyrus; CA: cornu ammonis

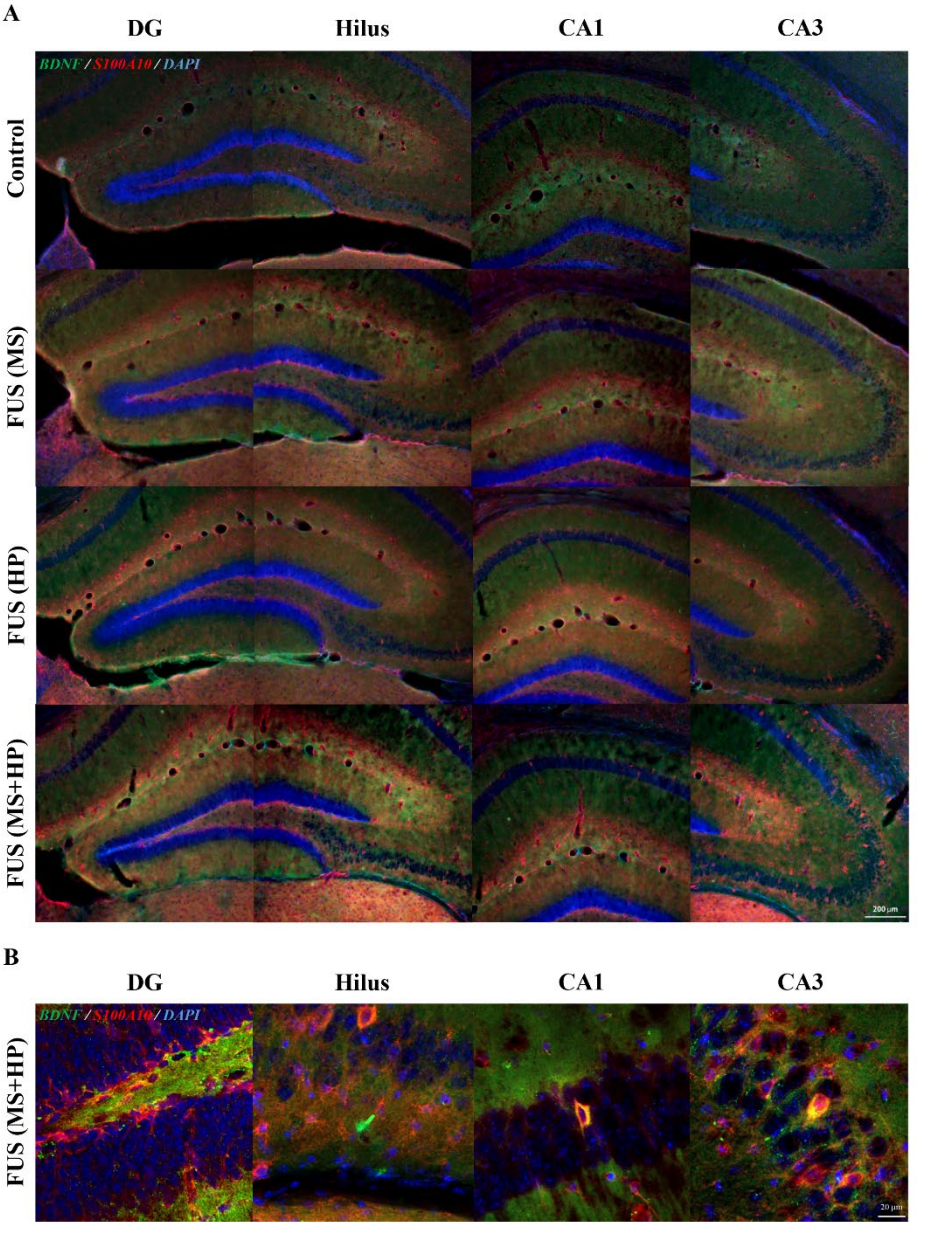

Figure 10. Co-staining BDNF and A2-type astrocytes. The A2 phenotype marker S100A10 (red) and BDNF (green) were co-stained and were most highly expressed in the focused ultrasound (FUS) medial septum + hippocampus

(MS+HP) group, especially compared to that of the control group (Figure 10A). The image was then visualized at 40× magnification (Figure 10B). The scale bar represents 200 μm (Figure 10A) and 20 μm (Figure 10B). DG: dentate gyrus; CA: cornu ammonis

4. Changes in the expression of neuronal activity and neurotrophic factors after FUS

The upregulation of BDNF/TrkB signaling by FUS modulation was confirmed (Figure 11). Proteolytic processing converts proBDNF into the mature form (mBDNF). TrkB binding to mBDNF activates the ERK1/2 and PI3K/Akt pathways to support synaptic plasticity and cell survival.[27]

As a result of western blot analysis of the FUS target area, the expression of mBDNF increased significantly in the HP (**p = 0.0092) and the MSHP groups (***p = 0.0003) compared to that of the control. It was confirmed that the level of TrkB expression also increased in the HP (*p = 0.0476) and MSHP groups (**p = 0086). This BDNF/TrkB signaling also affected Akt activation and its significance was confirmed in the MSHP group (*p = 0.013). Activation of the NMDA receptor, NR2B, in the MSHP group (*p = 0.0462) was also confirmed.

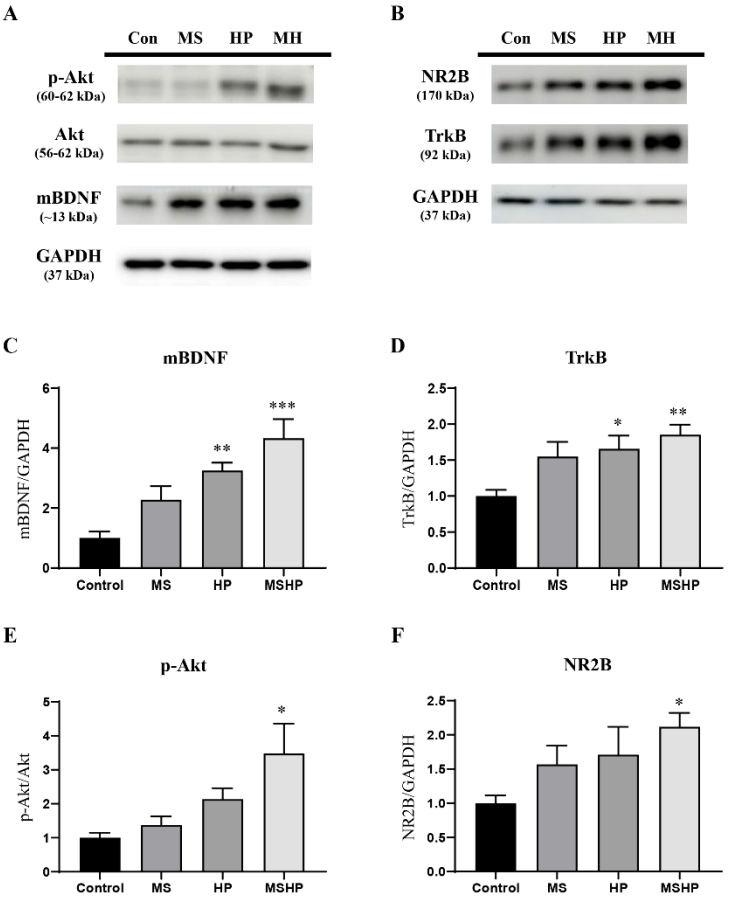

Figure 11. Expression levels of neurotrophic factors according to the FUS-targeted regions. (A) Representative results of western blotting with 12% sodium dodecyl sulfate-polyacrylamide gel electrophoresis (SDS-PAGE). (B) Representative results of western blotting with 8% SDS-PAGE gel. The expression levels of (C) mature brain-derived neurotrophic factor (mBDNF) and (D) tropomyosin receptor kinase B (TrkB) were increased in the hippocampus (HP) and medial septum + hippocampus (MSHP) groups. The (E) phosphorylated protein kinase B (p-Akt) and (F) N-methyl D-aspartate receptor

subtype 2B (NR2B) expression levels were elevated in the MSHP group. Data are expressed as the mean ± standard error of the mean (SEM) (n = 7 for each group). *$p < 0.05$, **$p < 0.01$, ***$p < 0.001$; One-way analysis of variance (ANOVA) with Tukey's multiple comparison test.

5. Changes in cognitive function according to the FUS-sonicated region

The effect of FUS modulation in the MS, HP, or MS+HP groups on spatial memory was evaluated using the Y-maze test. For each group, tests were performed at 1 hour, 1 day, 2 days, and 3 days after FUS treatment. As a result, the alternation rate increased overall in the FUS group compared to the control. However, there was no significant difference between the MS (Figure 12A) and HP groups (Figure 12B), and there was a statistically significant increase only in the Day 2 group (*p = 0.038) of the MS+HP group (Figure 12C).

AChE activity was quantified by the Ellman assay in the MS and HP (Figure 13). AChE activity was not significant in the MS (Figure 13A), while the activity increased in the HP of the FUS-treated groups compared to that of the control group (Figure 13B). The AChE activity in the FUS-treated regions also increased in the MS (*p = 0.0274), HP (**p = 0.0084), and MSHP groups (**p = 0.0011), respectively.

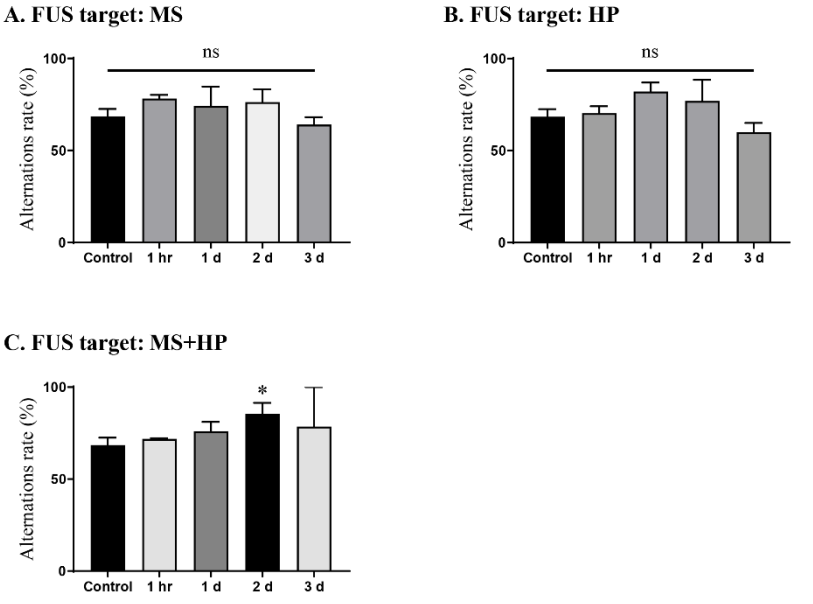

Figure 12. The effect of FUS modulation on cognitive function according to the FUS targets. Bar graphs show the spontaneous alternation rate according to the FUS-sonicated region. (A, B) There was no significant difference between the medial septum (MS) group and the hippocampus (HP) group. (C) Day 2 of the MS+HP group had an increased alternation rate. Data are expressed as the mean ± standard error of the mean (SEM) (n = 12 for each group, $*p < 0.05$). One-way analysis of variance (ANOVA) with Tukey's multiple comparison test were also performed.

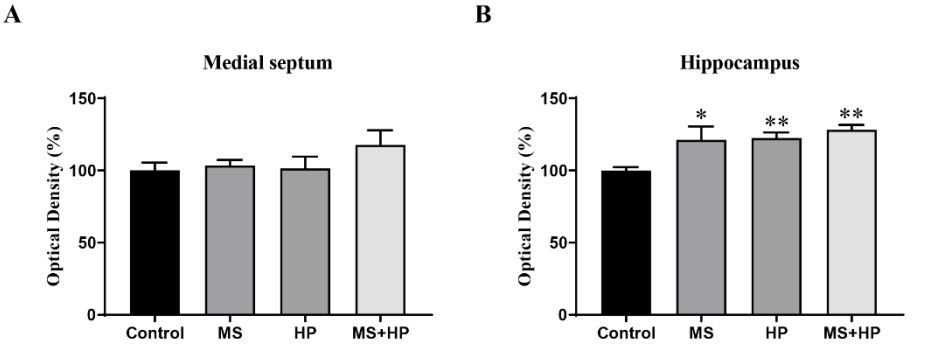

Figure 13. Change in acetylcholinesterase (AChE) activity by the FUS-sonicated regions. (A) There was no significant difference in AChE activity between any of the groups. (B) The AChE activity in the hippocampus of each FUS-treated group increased significantly. The AChE activity was expressed as the optical density at 405 nm. Values are represented as the mean ± standard error of the mean (SEM). *$p < 0.05$ and **$p < 0.01$ were considered as statistically significant compared to the control group.

Part 2. Modulation of the septo-hippocampal pathway in a 5xFAD mouse model of AD

6. Elevation of BDNF protein levels in astrocytes after FUS

Changes in BDNF expressed in astrocytes in the 5xFAD mice were confirmed through immunohistochemistry. As a result, it was confirmed that the BDNF/GFAP of the 5xFAD mice decreased compared to the LM control and increased in the 5xFAD mice group ultrasonically treated at the MS+HP regions compared to that of the untreated 5xFAD mice (Figure 14).

In addition, the expression of astrocytes according to the phenotype was also confirmed. The astrocyte expression of the FUS group remained unchanged when the A1 phenotypic marker C3 and BDNF were stained together (Figure 15). When the A2 phenotype marker S100A10 and BDNF were stained together, it was shown that the astrocyte expression in the 5xFAD + FUS group increased in comparison to that of the 5xFAD group (Figure 16A). Afterward, the image was enlarged to a 40× magnification (Figure 16B).

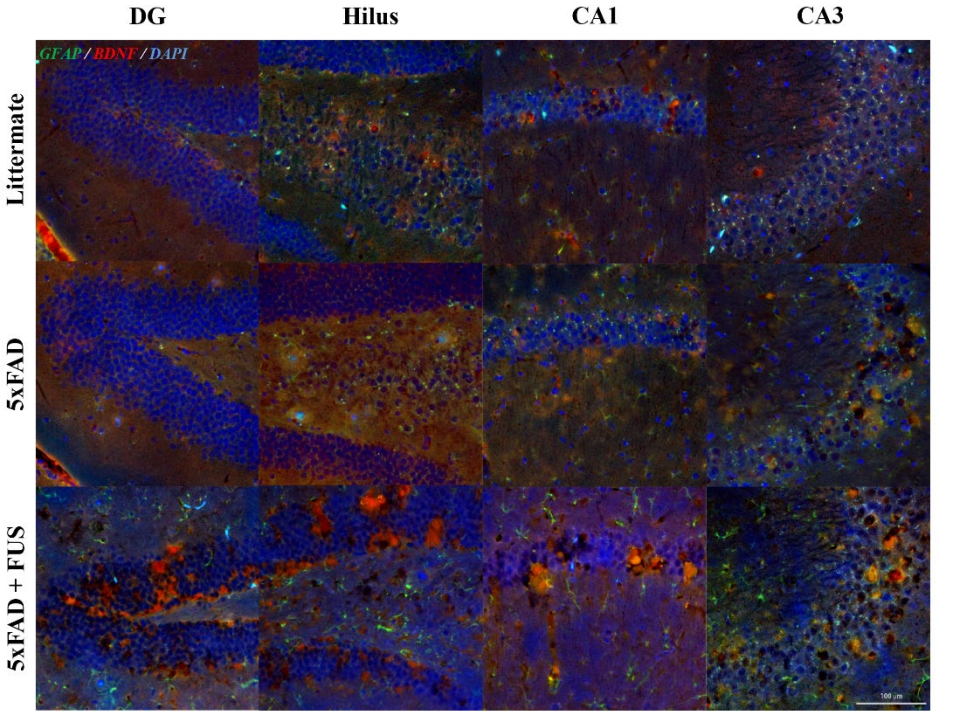

Figure 14. FUS improved the BDNF expression in astrocytes of 5xFAD mice. Co-staining of GFAP (green) and BDNF (red) after FUS in 5xFAD mice resulted in noticeably more expression in the FUS group than in the 5xFAD group. The scale bar represents 100 μm. DG: dentate gyrus; CA: cornu ammonis

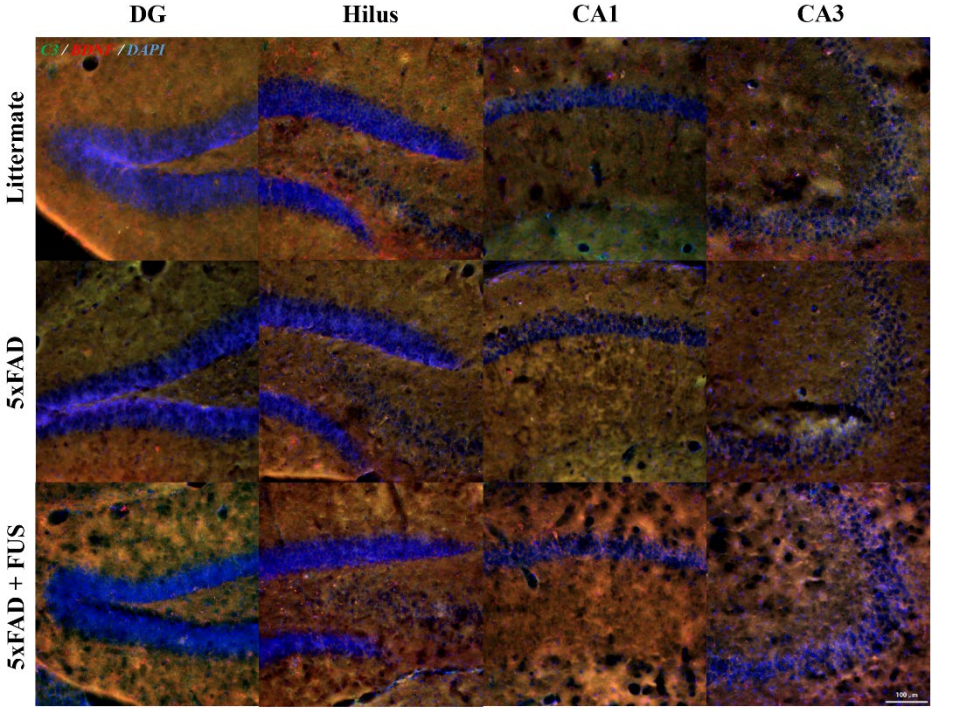

Figure 15. Co-staining of BDNF and A1 astrocytes after FUS in 5xFAD mice.

Changes in the expression of A1 astrocytes (C3 in green) were not confirmed after FUS in 5xFAD mice. The scale bar represents 100 μm. DG: dentate gyrus; CA: cornu ammonis

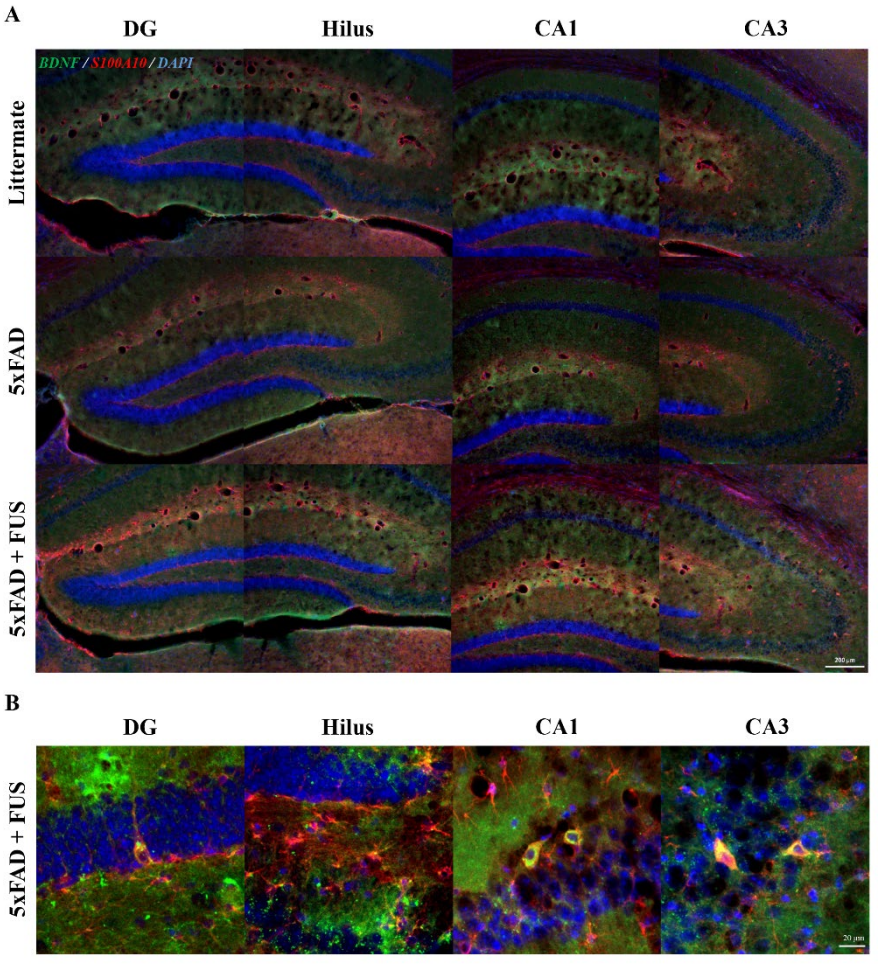

Figure 16. Changes in the expression of BDNF and A2 astrocytes after FUS in 5xFAD mice. The A2 phenotype marker S100A10 (red) and BDNF (green) were co-stained and were expressed in the 5xFAD + FUS group compared to the 5xFAD group (Figure 16A). Co-localization was identified by a 40-fold magnification. (Figure 16B). The scale bars represent 200 μm (Figure 16A) and 20 μm (Figure 16B). DG: dentate gyrus; CA: cornu ammonis

7. Activation of BDNF/TrkB and Akt signaling after FUS

The modulation of the MS and HP by FUS was found to increase BDNF/TrkB signaling (Figure 17). The PI3K/Akt pathway was activated by TrkB binding to mBDNF to enable synaptic plasticity and cell survival.[27]

As a result of western blot analysis, the expression of mBDNF decreased significantly in the TG group (**p = 0.0026) compared to that of the LM group and increased in the TG + FUS group (*p = 0.0264) compared to that of the TG group. It was confirmed that the level of expression of TrkB also decreased in the TG group (*p = 0.0404) compared to that of the LM group and increased in the TG +FUS group (*p = 00293) compared to that of the TG group. This BDNF/TrkB signaling also affected Akt activation and its significance was confirmed by Akt downregulation in the TG group (**p = 0.0028) compared to the LM group and Akt upregulation in the TG + FUS group (*p = 0.0189) compared to the TG group. The activation of NR2B, an NMDA receptor, also showed the same tendency. The expression of NR2B in the TG group decreased compared to that of the LM group (*p = 0.0194) and increased in the TG + FUS group (*p = 0.0418).

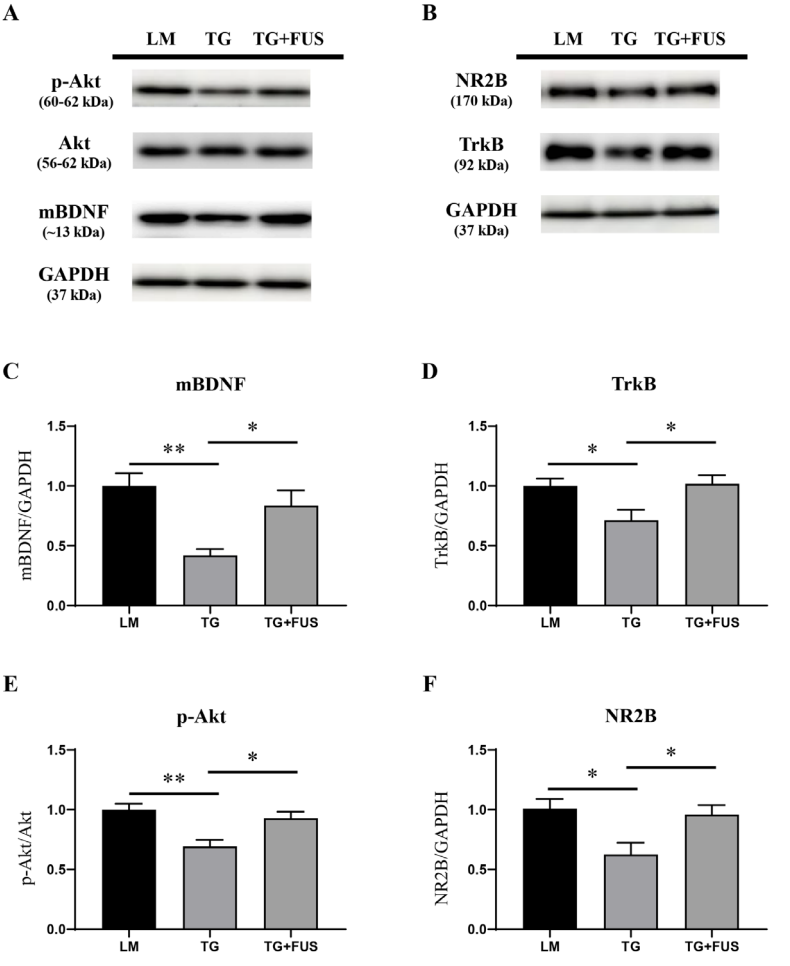

Figure 17. Comparison of the neurotrophic factors by FUS in 5xFAD mice. Representative results of western blotting with (A) 12% and (B) 8% sodium dodecyl sulfate-polyacrylamide gel electrophoresis (SDS-PAGE) gel. (C) mature brain-derived neurotrophic factor (mBDNF), (D) tropomyosin receptor kinase B (TrkB), (E) phosphorylated protein kinase B (p-Akt), and (F) N-methyl D-aspartate receptor subtype 2B (NR2B) expression in the TG group decreased compared to that of the littermate (LM) group but increased after FUS. Data are

expressed as the mean ± standard error of the mean (SEM) (n = 7 for each group, *$p < 0.05$, **$p < 0.01$). Statistical analysis was performed using one-way analysis of variance (ANOVA) with Tukey's multiple comparison test.

8. Cholinergic neuronal activity in AD by FUS modulation

The expression of choline acetyltransferase (ChAT) was evaluated by immunohistochemistry (IHC) (Figure 18). The number of ChAT-immunopositive neurons in the TG group was lower than that in the LM group. Additionally, the amount was increased in the TG + FUS compared to that of the TG group.

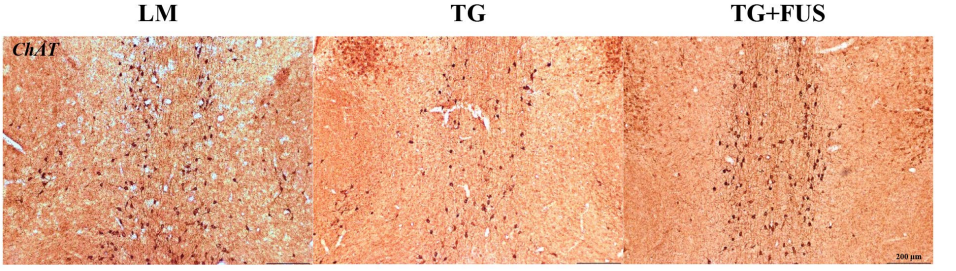

Figure 18. Representative images of choline acetyltransferase (ChAT)-positive cells. The expression of cholinergic cells was decreased in the transgenic (TG) group compared to that of the littermate (LM) control, but not in the focused ultrasound (FUS)-treated group. The scale bar represents 200 μm.

9. Neuroprotective effects of FUS modulation

AChE activity was quantified by the Ellman assay in the MS and HP (Figure 19). In the MS, AChE activity was significantly reduced in the TG group (****$p < 0.0001$) compared to that of the LM group. However, it was improved in the TG + FUS group (****$p < 0.0001$) compared to that of the TG group. In the HP, like in the MS, the AChE activity was reduced in the TG group (**$p = 0.0047$) compared to that of the LM group and was restored in the TG + FUS group (*$p = 0.0454$) compared to that of the TG group.

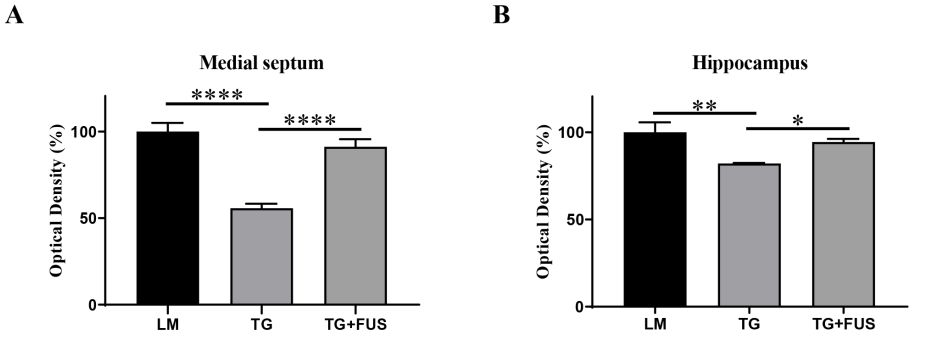

Figure 19. An increase in AChE activity by FUS in 5xFAD mice. (A) AChE activity in the medial septum. The level of AChE activity decreased in the transgenic (TG) group compared to that of the littermate (LM) control and increased in the TG + FUS group. (B) AChE activity in the hippocampus. The AChE activity in the TG group was decreased compared to that of the LM group but increased after FUS treatment. The AChE activity was expressed as the optical density at 405 nm. Values are represented as the mean ± standard error of the mean (SEM). *$p < 0.05$, **$p < 0.01$, and ****$p < 0.0001$ were considered statistically significant.

10. Improvement in cognitive function in 5xFAD mice

The effect of FUS modulation in the MS+HP of 5xFAD mice on spatial memory was evaluated using the Y-maze test. For each group, tests were performed at 1 hour, 1 day, 2 days, 3 days, and 4 days after FUS treatment. As a result, the alternation rate increased overall in the FUS group compared to that of the TG group (Figure 20A). There was also a significant difference in the TG group (**p = 0.013) compared to the LM group, and there were statistically significant increases in the Day 1 (*p = 0.0186) and Day 2 groups (**p = 0.0059). There was no significant difference in the total number of arm entries in the experimental groups (Figure 20B).

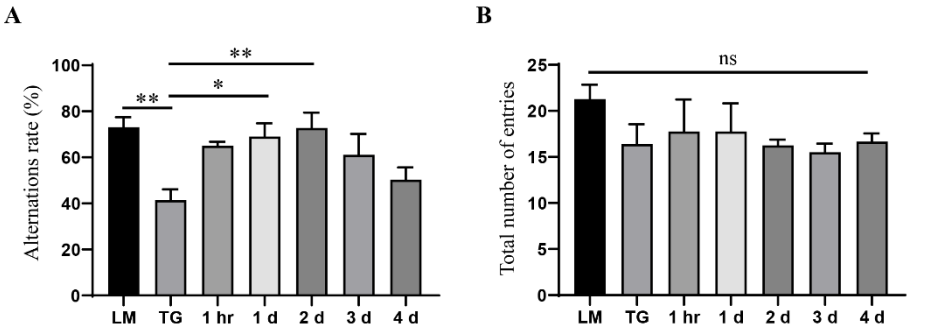

Figure 20. Effect of FUS modulation in the septo-hippocampal area of 5xFAD mice on cognitive function. (A) The bar graphs show the spontaneous alternation rate. The percentage of spontaneous change increased significantly on days 1 and 2 after FUS compared with that in the transgenic (TG) mice. (B) The number of arm entries exhibited no significant difference among any group of animals. Data are expressed as the mean ± standard error of the mean (SEM) (n = 10 for each group, *$p < 0.05$, **$p < 0.01$). Statistical analysis was performed using one-way analysis of variance (ANOVA) with Tukey's multiple comparison test.

IV. DISCUSSION

Alzheimer's disease (AD) is a neurodegenerative disorder characterized by cognitive decline and memory impairment, and it poses significant challenges for healthcare systems globally.[33] Current treatments mainly address symptoms with limited success in altering the disease's progression, thus necessitating innovative interventions to target the underlying mechanisms of AD and preserve cognitive function.[34] Recently, neuromodulation techniques have gained attention as potential AD treatments, with FUS emerging as a promising non-invasive method capable of precisely targeting specific brain regions.[35] FUS allows for controlled modulation of neural activity without invasive procedures or exogenous substances.[36] The septo-hippocampal area, vital for cognitive processes, was set as a FUS target in this study, as dysfunction and degeneration within this circuitry are prominent in AD pathology.[37] Moreover, the role of BDNF pathways in mediating cognitive enhancements after FUS treatment has been explored, offering a potential therapeutic mechanism. By investigating the impact of low-intensity FUS on the septo-hippocampal area and its effect on cognitive function in normal and AD mouse models, this study sheds light on the potential use of FUS as a targeted and effective therapeutic strategy for AD.

1. FUS modulation for cognitive enhancement in normal and AD mouse models

FUS neuromodulation offers adaptability and reversibility, allowing for personalized treatment approaches that can be adjusted based on individual responses and disease progression.[38] Moreover, its non-invasive and safe nature makes it accessible to a broader range of patients, including those who may not be suitable candidates for surgical interventions.[39]

Intriguingly, FUS neuromodulation has shown promise in improving cognitive function in normal mice. Studies on normal mice have demonstrated cognitive enhancements after FUS treatment, suggesting that FUS's positive effects on brain circuitry and neural activity could be harnessed to benefit individuals without AD.

The versatility of FUS neuromodulation in addressing both AD pathology and general cognitive enhancement highlights its broad therapeutic potential. By shedding light on the mechanisms underlying FUS-induced cognitive improvements in AD and normal mouse models, this research opens new possibilities for utilizing FUS to enhance brain function in various contexts. FUS has recently emerged as a promising non-invasive neuromodulation technique for AD treatment. Its precise targeting of specific brain regions with focused ultrasonic waves, without invasive procedures or exogenous substances, offers advantages over conventional interventions.[40]

2. Targeting the septo-hippocampal area with FUS

The septo-hippocampal pathway is a bidirectional neural connection between the septum and the HP. The septo-hippocampal pathway is crucial for memory and cognitive functions.[41] The cholinergic projections from the septal nuclei to the HP are involved in enhancing memory encoding and consolidation.[42] Acetylcholine release in the HP helps facilitate synaptic plasticity, which is essential for memory formation and learning.[43] Therefore, in this study, the MS was first stimulated with FUS to stimulate choline neurons projected into the HP. This could lead to the release of acetylcholine in the HP, which, as mentioned earlier, is important for memory formation and learning. By priming the HP with increased acetylcholine levels, subsequent stimulation of the HP may enhance synaptic plasticity and further potentiate memory-related processes.

Furthermore, FUS's capability to modulate neural activity with high spatial resolution makes the septo-hippocampal area an attractive target for AD treatment. This region plays a vital role in cognitive processes, including memory and learning, and is significantly affected by AD pathology.[44] By leveraging FUS to influence this circuitry, there is potential to enhance cognitive function.

3. Influence of FUS on BDNF pathways

The results of our study demonstrate a significant increase in BDNF expression in astrocytes following ultrasonic stimulation. Moreover, the upregulation of BDNF was accompanied by an increased expression of its associated receptors, TrkB and Akt, as well as the NMDA receptor subunit NR2B. These findings shed light on the potential mechanisms underlying the neurotrophic effects of ultrasonic stimulation and its implications for neurological disorders and brain plasticity.[45] Understanding the mechanisms underlying neuroprotection, such as BDNF-mediated signaling, could lead to novel therapeutic interventions for neurological disorders and brain injuries.[46,47]

The observed increase in BDNF expression in astrocytes is consistent with previous studies that have shown astrocytes as a source of BDNF in the brain.[23,45] This suggests that ultrasonic stimulation might induce BDNF release from astrocytes, contributing to the overall neurotrophic effects. BDNF is a key neurotrophin known to promote neuronal survival, growth, and synaptic plasticity, making it a critical factor in maintaining brain health and function.[48]

The concurrent increased expression of TrkB, the high-affinity receptor for BDNF, reinforces the likelihood of enhanced BDNF-TrkB signaling upon FUS stimulation. Activation of the TrkB pathway has been associated with various neuroprotective effects, including increased cell survival and neurite outgrowth.[46,49] Thus, the upregulation of TrkB expression suggests a potential mechanism through which ultrasonic stimulation could exert its neurotrophic

actions.

Furthermore, the increased expression of Akt, a downstream effector of the TrkB pathway, provides additional evidence of the activation of BDNF-mediated signaling cascades in response to FUS stimulation.[50] Akt is a serine/threonine kinase that is involved in cell survival and synaptic plasticity. Its upregulation may promote neuronal survival and enhance synaptic connectivity, contributing to the observed neurotrophic effects.[51]

Interestingly, our findings also revealed an increase in NR2B expression following ultrasonic stimulation. The NR2B subunit is a critical component of NMDA receptors, which play a crucial role in synaptic plasticity and learning.[52] The enhanced expression of NR2B suggests that FUS stimulation may influence NMDA receptor activity, potentially impacting synaptic plasticity and cognitive processes.

The collective evidence from our study suggests that ultrasonic stimulation elicits a complex neurotrophic response in astrocytes and neurons through the upregulation of BDNF-TrkB signaling, Akt activation, and enhanced NMDA receptor expression. These findings have significant implications for understanding the therapeutic potential of ultrasonic stimulation in various neurological disorders.

Neurological disorders, such as Alzheimer's disease and Parkinson's disease, which are characterized by impaired neurotrophic support, could potentially benefit from ultrasonic stimulation as a non-invasive and targeted approach to

boost BDNF levels and promote neuronal survival. Additionally, the observed increase in NR2B expression may suggest a role for ultrasonic stimulation in modulating synaptic plasticity and cognitive function, making it a promising avenue for enhancing learning and memory.

4. Neuroprotective effects of FUS on cholinergic neurons

AD is characterized by the progressive loss of cholinergic neurons, leading to a reduction in the acetylcholine (ACh) level, which is crucial for cognitive function. The 5xFAD mouse model is widely used to study AD due to its ability to recapitulate key pathological features of the disease, including Aβ plaque deposition and cholinergic neuron loss.[28,30]

In this study, we investigated the potential neuroprotective effects of ultrasonic stimulation on cholinergic neurons in the septo-hippocampal area of 5xFAD mice. The septo-hippocampal cholinergic pathway involves cholinergic neurons, which release ACh, an important neurotransmitter responsible for various cognitive functions.[53] These neurons are found in the septal nuclei and project their axons to the HP, specifically to the subfields known as the dentate gyrus (DG) and cornu ammonis (CA) regions.[21] This cholinergic projection is essential for modulating hippocampal activity and promoting memory formation and retrieval.[44,54] Our findings demonstrate that FUS can rescue cholinergic neurons from degeneration, leading to increased cholinergic neuron survival in the stimulated group compared to the non-stimulated 5xFAD mice.

The activity of AChE, the enzyme responsible for degrading ACh, is significantly reduced in the 5xFAD mice due to the lower availability of ACh, resulting from cholinergic neuron loss. Interestingly, the ultrasonic stimulation group exhibited increased AChE activity compared to the non-stimulated 5xFAD mice. This unexpected observation could be attributed to the

preservation of cholinergic neurons through neuroprotective mechanisms induced by the ultrasonic waves. The survival of cholinergic neurons in response to ultrasonic stimulation may lead to higher ACh release and subsequently trigger a compensatory upregulation of AChE activity to maintain cholinergic neurotransmission.

5. Implications for AD therapeutics

This study provides valuable insights into the molecular and cellular effects of ultrasonic stimulation on astrocytes and neurons. The upregulation of BDNF, TrkB, Akt, and NR2B expression points towards the activation of neurotrophic and synaptic plasticity pathways. In addition, the neuroprotective effects of ultrasonic stimulation on cholinergic neurons in the 5xFAD mouse model provide valuable insights into potential therapeutic strategies for AD.

However, it is essential to acknowledge that the field of FUS neuromodulation for AD and cognitive enhancement is still in its early stages, and further research is needed to fully understand its safety, long-term efficacy, and the optimal parameters for treatment. Rigorous clinical trials with larger sample sizes and longer follow-up periods are necessary to assess FUS's potential as a viable therapeutic option for AD patients and its potential for cognitive enhancement in non-AD individuals.

V. CONCLUSION

This study aimed to investigate the effects of FUS on the septo-hippocampal region and cognitive function in both normal and AD mouse models. FUS neuromodulation holds promise as a non-invasive and versatile approach for treating AD and enhancing cognitive function.

In Part 1, optimal ultrasonic parameters that are safe and effective in normal mice were established. An improvement in cognitive function was observed in the group where the septo-hippocampal area of general mice was stimulated. The potential benefits of these results suggest a broader application of FUS in improving cognitive function for the general public. In Part 2, the recovery of cognitive function was confirmed in the group of AD mice with ultrasonically treated septo-hippocampal areas. Moreover, this study highlights the neuroprotective potential of ultrasonic stimulation on cholinergic neurons in the 5xFAD mouse model of AD. These findings open new avenues for exploring novel therapeutic strategies that aim to preserve cholinergic neurotransmission and cognitive function in AD.

However, further research and rigorous clinical trials are required to fully explore the safety, long-term efficacy, and optimal parameters of FUS neuromodulation for AD and general cognitive enhancement. As research in this field continues to evolve, FUS may hold the key to a brighter future for individuals affected by AD and those seeking to optimize their cognitive capabilities.

REFERENCES

1. Boyle PA, Yu L, Leurgans SE, Wilson RS, Brookmeyer R, Schneider JA, et al. Attributable risk of Alzheimer's dementia attributed to age-related neuropathologies. *Ann Neurol.* 2019;85(1):114-124.
2. Karran E, De Strooper B. The amyloid hypothesis in Alzheimer disease: new insights from new therapeutics. *Nature Reviews Drug Discovery.* 2022;21(4):306-318.
3. Karran E, Mercken M, De Strooper B. The amyloid cascade hypothesis for Alzheimer's disease: an appraisal for the development of therapeutics. *Nat Rev Drug Discov.* 2011;10(9):698-712.
4. Lorenzini L, Ingala S, Collij LE, Wottschel V, Haller S, Blennow K, et al. Eigenvector centrality dynamics are related to Alzheimer's disease pathological changes in non-demented individuals. *Brain Commun.* 2023;5(3):fcad088.
5. Schneider LS, Dagerman KS, Higgins JP, McShane R. Lack of evidence for the efficacy of memantine in mild Alzheimer disease. *Archives of neurology.* 2011;68(8):991-998.
6. Aisen PS, Davis KL, Berg JD, Schafer K, Campbell K, Thomas RG, et al. A randomized controlled trial of prednisone in Alzheimer’s disease. *Neurology.* 2000;54(3):588-593.
7. Cheyuo C, Germann J, Yamamoto K, Vetkas A, Loh A, Sarica C, et al. Connectomic neuromodulation for Alzheimer’s disease: A systematic review and meta-analysis of invasive and non-invasive techniques. *Translational Psychiatry.* 2022;12(1):490.
8. Pople CB, Meng Y, Li DZ, Bigioni L, Davidson B, Vecchio LM et al. Neuromodulation in the Treatment of Alzheimer’s Disease: Current and Emerging Approaches. *Journal of Alzheimer's Disease.*

2020;78(4):1299-1313.

9. Chen LM, Yang P-F, Mishra A, Phipps MA, Manuel T, Sigona M, et al. MRI-guided focused ultrasound neuromodulation of deep brain regions and circuits with real time feedback. *Brain Stimulation*. 2023;16(1):117-118.
10. Beisteiner R, Hallett M, Lozano AM. Ultrasound Neuromodulation as a New Brain Therapy. *Adv Sci (Weinh).* 2023;10(14):e2205634.
11. Chen Y, Li Y, Du M, Yu J, Gao F, Yuan Z, et al. Ultrasound Neuromodulation: Integrating Medicine and Engineering for Neurological Disease Treatment. *BIO Integration.* 2021;2(4):169-179.
12. King RL, Brown JR, Newsome WT, Pauly KB. Effective Parameters for Ultrasound-Induced In Vivo Neurostimulation. *Ultrasound in medicine & biology.* 2013;39(2):312-331.
13. Kim H, Chiu A, Lee SD, Fischer K, Yoo S-S. Focused Ultrasound-mediated Non-invasive Brain Stimulation: Examination of Sonication Parameters. *Brain stimulation.* 2014;7(5):748-756.
14. Yoo S-S, Bystritsky A, Lee J-H, Zhang Y, Fischer K, Min B-K, et al. Focused ultrasound modulates region-specific brain activity. *NeuroImage.* 2011;56(3):1267-1275.
15. Tyler WJ, Tufail Y, Finsterwald M, Tauchmann ML, Olson EJ, Majestic C. Remote excitation of neuronal circuits using low-intensity, low-frequency ultrasound. *PloS one.* 2008;3(10):e3511.
16. Baek H, Pahk KJ, Kim MJ, Youn I, Kim H. Modulation of Cerebellar Cortical Plasticity Using Low-Intensity Focused Ultrasound for Poststroke Sensorimotor Function Recovery. *Neurorehabilitation and neural repair.* 2018;32(9):777-787.
17. Yoo S-S, Kim H, Min B-K, Franck E, Park S. Transcranial focused ultrasound to the thalamus alters anesthesia time in rats. *Neuroreport.* 2011;22(15):783-787.

18. Younan Y, Deffieux T, Larrat B, Fink M, Tanter M, Aubry JF. Influence of the pressure field distribution in transcranial ultrasonic neurostimulation. *Medical physics.* 2013;40(8):082902.
19. Baek H, Pahk KJ, Kim H. A review of low-intensity focused ultrasound for neuromodulation. *Biomedical Engineering Letters.* 2017;7(2):135-142.
20. Price DL, Koliatsos VE, Clatterbuck RC. Cholinergic systems: human diseases, animal models, and prospects for therapy. *Progress in brain research.* 1993;98:51-60.
21. Müller C, Remy S. Septo–hippocampal interaction. *Cell and Tissue Research.* 2018;373(3):565-575.
22. Krügel U, Bigl V, Eschrich K, Bigl M. Deafferentation of the septo-hippocampal pathway in rats as a model of the metabolic events in Alzheimer's disease. *International Journal of Developmental Neuroscience.* 2001;19(3):263-277.
23. Yang FY, Lu WW, Lin WT, Chang CW, Huang SL. Enhancement of Neurotrophic Factors in Astrocyte for Neuroprotective Effects in Brain Disorders Using Low-intensity Pulsed Ultrasound Stimulation. *Brain stimulation.* 2015;8(3):465-473.
24. Kowiański P, Lietzau G, Czuba E, Waśkow M, Steliga A, Moryś J. BDNF: A Key Factor with Multipotent Impact on Brain Signaling and Synaptic Plasticity. *Cellular and Molecular Neurobiology.* 2018;38(3):579-593.
25. D'Angelo B, Santucci S, Benedetti E, Di Loreto S, Phani RA, Falone S, et al. Cerium Oxide Nanoparticles Trigger Neuronal Survival in a Human Alzheimer Disease Model By Modulating BDNF Pathway. *Current Nanoscience.* 2009;5(2):167-176.
26. Lin WT, Chen RC, Lu WW, Liu SH, Yang FY. Protective effects of low-intensity pulsed ultrasound on aluminum-induced cerebral damage in Alzheimer's disease rat model. *Scientific reports.* 2015;5:9671.

27. Numakawa T, Odaka H. Brain-Derived Neurotrophic Factor Signaling in the Pathophysiology of Alzheimer's Disease: Beneficial Effects of Flavonoids for Neuroprotection. *Int J Mol Sci.* 2021;22(11).

28. Oakley H, Cole SL, Logan S, Maus E, Shao P, Craft J, et al. Intraneuronal beta-amyloid aggregates, neurodegeneration, and neuron loss in transgenic mice with five familial Alzheimer's disease mutations: potential factors in amyloid plaque formation. *J neuroscience.* 2006;26(40):10129-10140.

29. Qiu Z, Kala S, Guo J, Xian Q, Zhu J, Zhu T, et al. Targeted Neurostimulation in Mouse Brains with Non-invasive Ultrasound. *Cell Rep.* 2020;32(7):108033.

30. Devi L, Ohno M. Phospho-eIF2α level is important for determining abilities of BACE1 reduction to rescue cholinergic neurodegeneration and memory defects in 5XFAD mice. *PloS one.* 2010;5(9):e12974.

31. Eimer WA, Vassar R. Neuron loss in the 5XFAD mouse model of Alzheimer's disease correlates with intraneuronal Aβ42 accumulation and Caspase-3 activation. *Mol Neurodegener.* 2013;8:2.

32. Ellman GL, Courtney KD, Andres V, Featherstone RM. A new and rapid colorimetric determination of acetylcholinesterase activity. *Biochemical Pharmacology.* 1961;7(2):88-95.

33. Grober E, Hall CB, Lipton RB, Zonderman AB, Resnick SM, Kawas C. Memory impairment, executive dysfunction, and intellectual decline in preclinical Alzheimer's disease. *Journal of the International Neuropsychological Society.* 2008;14(2):266-278.

34. Pardo-Moreno T, González-Acedo A, Rivas-Domínguez A, García-Morales V, García-Cozar FJ, Ramos-Rodríguez JJ, et al. Therapeutic Approach to Alzheimer's Disease: Current Treatments and New Perspectives. *Pharmaceutics.* 2022;14(6).

35. Darrow DP. Focused Ultrasound for Neuromodulation.

Neurotherapeutics. 2019;16(1):88-99.

36. Tyler WJ, Lani SW, Hwang. Ultrasonic modulation of neural circuit activity. *Curr Opin Neurobiol.* 2018;50:222-231.
37. Schliebs R, Arendt T. The cholinergic system in aging and neuronal degeneration. *Behavioural Brain Research.* 2011;221(2):555-563.
38. Tufail Y, Matyushov A, Baldwin N, Tauchmann ML, Georges J, Yoshihiro A, et al. Transcranial pulsed ultrasound stimulates intact brain circuits. *Neuron.* 2010;66(5):681-694.
39. Zhang T, Pan N, Wang Y, Liu C, Hu S. Transcranial Focused Ultrasound Neuromodulation: A Review of the Excitatory and Inhibitory Effects on Brain Activity in Human and Animals. *Front Hum Neurosci.* 2021;15:749162.
40. Fini M, Tyler WJ. Transcranial focused ultrasound: a new tool for non-invasive neuromodulation. *Int Rev Psychiatry.* 2017;29(2):168-177.
41. Niewiadomska G, Baksalerska-Pazera M, Riedel G. The septo-hippocampal system, learning and recovery of function. *Progress in Neuro-Psychopharmacology and Biological Psychiatry.* 2009;33(5):791-805.
42. Krnjević K, Ropert N. Septo-hippocampal pathway modulates hippocampal activity by a cholinergic mechanism. *Can J Physiol Pharmacol.* 1981;59(8):911-914.
43. Hasselmo ME. Neuromodulation: acetylcholine and memory consolidation. *Trends Cogn Sci.* 1999;3(9):351-359.
44. Khakpai F, Nasehi M, Haeri-Rohani A, Eidi A, Zarrindast MR. Septo-hippocampo-septal loop and memory formation. *Basic and clinical neuroscience.* 2013;4(1):5-23.
45. Liu SH, Lai YL, Chen BL, Yang FY. Ultrasound Enhances the Expression of Brain-Derived Neurotrophic Factor in Astrocyte Through Activation of TrkB-Akt and Calcium-CaMK Signaling Pathways. *Cerebral cortex*

(New York, NY : 1991). 2017;27(6):3152-3160.

46. Yamada K, Nabeshima T. Brain-Derived Neurotrophic Factor/TrkB Signaling in Memory Processes. *Journal of Pharmacological Sciences.* 2003;91(4):267-270.
47. Colucci-D'Amato L, Speranza L, Volpicelli F. Neurotrophic Factor BDNF, Physiological Functions and Therapeutic Potential in Depression, Neurodegeneration and Brain Cancer. *Int J Mol Sci.* 2020;21(20).
48. Cunha C, Brambilla R, Thomas KL. A simple role for BDNF in learning and memory? *Front Mol Neurosci.* 2010;3:1.
49. Numakawa T, Kajihara R. Neurotrophins and Other Growth Factors in the Pathogenesis of Alzheimer's Disease. *Life (Basel).* 2023;13(3).
50. Zarneshan SN, Fakhri S, Khan H. Targeting Akt/CREB/BDNF signaling pathway by ginsenosides in neurodegenerative diseases: A mechanistic approach. *Pharmacological Research.* 2022;177:106099.
51. Brunet A, Datta SR, Greenberg ME. Transcription-dependent and -independent control of neuronal survival by the PI3K–Akt signaling pathway. *Current Opinion in Neurobiology.* 2001;11(3):297-305.
52. Zhou Y, Takahashi E, Li W, Halt A, Wiltgen B, Ehninger D, et al. Interactions between the NR2B Receptor and CaMKII Modulate Synaptic Plasticity and Spatial Learning. *J Neuroscience.* 2007;27(50):13843-13853.
53. Lauder JM, Schambra UB. Morphogenetic roles of acetylcholine. *Environ Health Perspect.* 1999;107 Suppl 1(Suppl 1):65-69.
54. Deiana S, Platt B, Riedel G. The cholinergic system and spatial learning. *Behavioural Brain Research.* 2011;221(2):389-411.

ABSTRACT (IN KOREAN)

알츠하이머병 모델에서 집속초음파에 의한 중격-해마 자극 후 향상된 기억 기능

<지도교수 장 진 우>

연세대학교 대학원 의과학과

서 영 희

알츠하이머병은 인지 저하, 기억력 손실 및 행동 장애를 특징으로 하는 신경 퇴행성 질환이다. 세계 인구의 고령화와 함께 알츠하이머병의 발병률은 계속 증가하여 전 세계적인 의료 분야에 상당한 도전 과제로 제시된다. 알츠하이머병에 대한 현재의 치료적 접근법은 주로 증상을 관리하고 일시적인 완화를 제공하는 데 초점을 맞추고 있으며, 근본적인 질병 진행의 치료를 성공하는 데는 제한적이다. 따라서 인지 기능을 보존하거나 향상시키기 위해 근본적인 병리학적 메커니즘을 대상으로 하는 혁신적인 개입이 절실히 필요하다.

최근 신경 조절 기술은 알츠하이머병 치료를 위한 유망한 방법으로 부상하고 있다. 이러한 기술 중 집속초음파는 높은 공간 해상도로 특정 뇌 영역을 정확하게 목표로 할 수 있는 비침습적 신경 조절 기술로 주목을 받고 있다. 두개골의

손상과 같은 침습적 절차나 외인성 물질의 투여 없이도 정밀하고 제어된 신경 조절을 가능하게 한다. 이러한 집속초음파의 자극은 신경 활동에 영향을 미치는 잠재력을 보여주었고, 질병의 발병과 관련된 복잡한 뇌 회로를 해결하기 위한 새로운 접근법을 제공했다. 또한 집속초음파는 반복적이고 가역적인 신경 조절을 허용하여 치료 전략에 이점을 제시하고 비가역적 개입과 관련된 부작용의 위험을 잠재적으로 줄인다.

본 연구에서는 저강도 집속초음파를 사용하여 내측 중격과 해마 부위를 자극하고 행동 평가와 분자생물학적 측정을 통해 인지 기능을 평가했다. 내측 중격과 해마의 회로는 인지 과정에서 중요한 역할을 하며, 이들의 기능 장애는 알츠하이머병의 병리학적 특징이다.

연구 결과에서 주목할 만한 것은 정상 동물과 알츠하이머병 모델 모두 집속초음파 치료 후 상당한 인지적 개선을 보였으며, 이는 인지기능 개선의 새로운 치료 전략의 가능성을 보여주었다. 기본 메커니즘을 설명하기 위해 관찰된 인지적 향상을 매개하는 뇌 유래 신경재생인자와 이와 관련된 경로의 인자들의 발현이 증가하였다. 신경세포 보호와 시냅스 가소성의 핵심 단백질인 뇌 유래 신경재생인자는 별아교세포에서 특히 증가하였고, 이 경로와 관련된 TrkB, Akt와 NMDAR도 초음파 자극 후 유의미하게 증가했다. 또한, 흥미롭게도 알츠하이머병 모델에서 감소 되어있던 ChAT 세포들은 집속초음파 그룹에서 회복되어 있었으며, AChE도

유의미하게 회복됨을 확인했다. 따라서 집속초음파에 의한 내측 중격과 해마 영역의 신경 조절이 알츠하이머병에서 인지 기능을 향상시킬 가능성을 가지고 있음을 시사한다.

본 연구에서는 기억 기능의 향상을 위한 집속초음파의 신경 조절을 통해 그 효과를 확인하고 알츠하이머병의 치료 가능성을 제시한다. 그러나 기억력 향상을 위한 집속초음파의 신경 조절 분야는 아직 초기 단계이며, 안전성, 장기 효과 및 치료를 위한 최적의 매개 변수를 완전히 이해하기 위해서는 추가 연구가 필요하다.

핵심되는 말 : 알츠하이머병, 집속초음파, 중격-해마 경로, 뇌유래 신경영양인자, 인지기능

PUBLICATION LIST

1. Lee J, Chang WS, Shin J, Seo Y, Kong C, Song B-W, et al. Non-invasively enhanced intracranial transplantation of mesenchymal stem cells using focused ultrasound mediated by overexpression of cell-adhesion molecules. *Stem Cell Res.* 2020;43:101726.

2. Ko K, Seo Y, Im S, Lee H, Park JY, Chang WS, et al. Ex Vivo Raman Spectroscopy Measurement of a Mouse Model of Alzheimer's Disease. *Korean Journal of Optics and Photonics*. 2022;331-337.

3. Seo Y, Han S, Song B-W, Chang JW, Na YC, Chang WS. Endogenous Neural Stem Cell Activation after Low-Intensity Focused Ultrasound-Induced Blood–Brain Barrier Modulation. *Int J Mol Sci.* 2023;24(6):5712.